Production of $f_0(1710)$, $f_0(1500)$, and $f_0(1370)$ in J/ψ hadronic decays

Frank E. Close[1,*] and Qiang Zhao[2,†]

[1]*Department of Theoretical Physics, University of Oxford, Keble Road, Oxford OX1 3NP, United Kingdom*
[2]*Department of Physics, University of Surrey, Guildford GU2 7XH, United Kingdom*

A coherent study of the production of f_0^i [$i = 1, 2, 3$ corresponding to $f_0(1710)$, $f_0(1500)$, and $f_0(1370)$] in $J/\psi \to V f_0 \to VPP$ is reported based on a previously proposed glueball and $Q\bar{Q}$ nonet mixing scheme, and a factorization for the decay of $J/\psi \to V f_0^i$, where V denotes the isoscalar vector mesons ϕ and ω, and P denotes pseudoscalar mesons. The results show that the J/ψ decays are very sensitive to the structure of those scalar mesons, and suggest a glueball in the 1.5–1.7 GeV region, in line with lattice QCD. The presence of significant glueball mixings in the scalar wave functions produces peculiar patterns in the branching ratios for $J/\psi \to V f_0^i \to VPP$, which are in good agreement with the recently published experimental data from the BES Collaboration.

PACS numbers: 13.25.Gv, 12.39.Mk, 12.39.St

I. INTRODUCTION

Although explicit evidence for a pure glueball state has never been confirmed in the spectroscopy of isoscalar mesons, experimental data are consistent with the scenario that a glueball should have significant mixings with quarkonia in the formation of some of those isoscalar mesons. This is expected to be especially important in the scalar mesons [1]. It is hence interesting to explore those mechanisms of isoscalar meson production which are sensitive to their glueball contents. Recently, Brodsky *et al.* [2] proposed a possible production mechanism for glueball states in $e^+ e^- \to \gamma^* \to J/\psi G_J$, where glueball production in the same mass region as the scalar charmonia (η_c and χ_{c0}) would contribute to the events observed in $e^+ e^- \to \gamma^* \to J/\psi X$ at Belle [3]. In contrast to the above prediction for a glueball of about 3 GeV, lattice QCD [4,5] and other phenomenological studies [6–8] suggest the lightest glueball mass at 1.5–1.7 GeV. Some analyses identify the lowest 0^+ glueball with the $f_0(1500)$ [7,9,10], while even lower glueball masses have been suggested in the literature [11]. It is thus natural to concentrate on this energy region and explore glueball production and possible mixings with quarkonia in the low-lying scalars, in particular, the three states f_0^i, where $i = 1, 2$ and 3 correspond to $f_0(1710)$, $f_0(1500)$ and $f_0(1370)$, respectively.

In Refs. [7,8], Close *et al.* proposed a flavor mixing scheme to produce the three f_0 states among the glueball G, flavor nonet $s\bar{s}$ and $n\bar{n}$. It hence relates the decays $f_0^i \to PP$, where P denotes pseudoscalar mesons (π, K, η, η'), to the mixing angles between G, $s\bar{s}$ and $n\bar{n}$. Since the mixing scheme is sensitive to the experimental data for $f_0^i \to PP$, their results not only provided a prescription for understanding the data from WA102 [12], but also highlighted the importance of the possible glueball contents in both $f_0(1500)$ and $f_0(1710)$, while the $f_0(1370)$ was dominated

by the $n\bar{n}$ component. In this scheme, the pattern of the mass matrix will be determined by the relative mass positions of G, $s\bar{s}$ and $n\bar{n}$. Therefore, for the pure glueball G it is crucial to compare with the lattice QCD predictions.

Independent production processes are required to examine such a glueball-$Q\bar{Q}$ mixing mechanism and provide more decisive evidence for the existence of the glueball contents in some of the f_0 states. At the Beijing Spectrometer (BES) the f_0 states have now been observed in both J/ψ radiative and hadronic decays, and interesting signals of these scalars have been reported [13–15]. In particular, the data show that these states behave contrary to expectations based on naive application of the Okubo-Zweig-Iizuka rule [16] in J/ψ decays [17]: (i) the $f_0(1370)$ has been seen clearly in $J/\psi \to \phi\pi\pi$, but not in $J/\psi \to \omega\pi\pi$; (ii) there is no peak of the $f_0(1500)$ directly seen in $J/\psi \to \phi K\bar{K}$, $\omega K\bar{K}$, $\phi\pi\pi$, $\omega\pi\pi$, though its production in proton-proton scattering is quite clear [12]; (iii) the $f_0(1710)$ is observed clearly in both $J/\psi \to \phi K\bar{K}$ and $J/\psi \to \omega K\bar{K}$, but with $\text{BR}_{J/\psi \to \omega f_0(1710) \to \omega K\bar{K}}/\text{BR}_{J/\psi \to \phi f_0(1710) \to \phi K\bar{K}} \simeq 6$, which is against a simple $s\bar{s}$ configuration for this state. The $f_0(1710)$ is not seen in $\phi\pi\pi$ and $\omega\pi\pi$, which is understandable due to its small branching ratio to $\pi\pi$. These observations hence raise questions about the configuration of the f_0 states, and also about their production mechanism in the J/ψ hadronic decays. BES also claims observations of another scalar $f_0(1790)$, which is distinct from the $f_0(1710)$. We will comment on this state in the last section, based on our results for the $f_0^{1,2,3}$.

An estimate of the low-lying glueball production rate has been made by extrapolating the perturbative QCD (pQCD) approach of Ref. [2] to the J/ψ energy region [18]. By studying $e^+ e^- \to J/\psi \to \phi G$ there, we showed that the glueball production rate can be approximately normalized in terms of the ideal $s\bar{s}(1S)$ state production. One of the results of the present paper will be to extract from the data the effective branching ratios for $J/\psi \to VG$.

───────────
*Email address: F.Close1@physics.ox.ac.uk
†Email address: Qiang.Zhao@surrey.ac.uk

In what follows, first we shall revisit the glueball-$Q\bar{Q}$ mixings in these three scalar f_0^i mesons, and clarify quantitatively the sensitivity of the mass matrix pattern to the available experimental data from WA102 [12] and BES [13,14]. We will then explore the implications of the glueball-$Q\bar{Q}$ mixings in the f_0^i productions in $J/\psi \rightarrow V f_0^i$, and compare the results with the recent experimental data from BES [13,14]. Conclusions about the f_0^i properties and their "puzzling" behaviors in the J/ψ decays will then be drawn.

II. THE THEORETICAL MODEL

A. Glueball and $Q\bar{Q}$ mixing

References [7,8] proposed a flavor mixing scheme for the three scalars $f_0^{1,2,3}$ corresponding to $f_0(1710)$, $f_0(1500)$ and $f_0(1370)$, respectively. In the basis of $|G\rangle = |gg\rangle$, $|s\bar{s}\rangle$ and $|n\bar{n}\rangle \equiv |u\bar{u} + d\bar{d}\rangle/\sqrt{2}$, the mass matrix for the glueball-quarkonia mixing can be written as

$$M = \begin{pmatrix} M_G & f & \sqrt{2}f \\ f & M_{s\bar{s}} & 0 \\ \sqrt{2}f & 0 & M_{n\bar{n}} \end{pmatrix}, \quad (1)$$

where M_G, $M_{s\bar{s}}$ and $M_{n\bar{n}}$ represent the masses of the pure states $|G\rangle$, $|s\bar{s}\rangle$, and $|n\bar{n}\rangle$, respectively. The parameter f is the flavor independent mixing strength between the glueball and quarkonia, and leads to the mixture of $|G\rangle$, $|s\bar{s}\rangle$, and $|n\bar{n}\rangle$ to form the physical f_0^i states. It can be expressed as $f \equiv \langle s\bar{s}|\hat{V}|G\rangle = \langle n\bar{n}|\hat{V}|G\rangle/\sqrt{2}$, where $\hat{V}$ is the potential causing such a mixing.

Treating $f_0(1710)$, $f_0(1500)$ and $f_0(1370)$ as the eigenstates of the mass matrix M with the eigenvalues of the physical resonance masses M_1, M_2 and M_3, respectively, we can then express these f_0 states as

$$\begin{pmatrix} |f_0(1710)\rangle \\ |f_0(1500)\rangle \\ |f_0(1370)\rangle \end{pmatrix} = \begin{pmatrix} x_1 & y_1 & z_1 \\ x_2 & y_2 & z_2 \\ x_3 & y_3 & z_3 \end{pmatrix} \begin{pmatrix} |G\rangle \\ |s\bar{s}\rangle \\ |n\bar{n}\rangle \end{pmatrix}, \quad (2)$$

where x_i, y_i and z_i are the mixing matrix elements determined by the perturbative transitions [7,8].

The decay of $f_0^i \rightarrow PP$ can then be factorized into contributions from three fundamental processes [8]:

(i) the direct coupling of the quarkonia component of the three f_0 states to the final pseudoscalar meson pairs;

(ii) the coupling of the glueball component of the three f_0 states to the pseudoscalar meson pairs;

(iii) the direct coupling of the glueball component to the gluonic component of the final state isoscalar meson pairs.

The coupling strength of (ii) is denoted by parameter r_2 relative to the coupling of (i); analogously, parameter r_3 is introduced to account for the coupling strength of (iii) relative to (i). In contrast to Ref. [8], we make here the more natural assumption that the G component of f_0 states couples to the flavor singlet $Q\bar{Q}$ component of the η and η'. Taking into account the η-η' mixing, the factorization for $f_0 \rightarrow PP$ is presented in Table I.

B. The production of f_0^i states in $J/\psi \rightarrow V f_0^i$

By defining the transition amplitudes via a potential V_ϕ,

$$M_{\phi G} \equiv \langle G|V_\phi|J/\psi\rangle, \qquad M_{\phi(s\bar{s})} \equiv \langle s\bar{s}|V_\phi|J/\psi\rangle,$$
$$M_{\phi(n\bar{n})} \equiv \langle n\bar{n}|V_\phi|J/\psi\rangle, \quad (3)$$

we can then express the transition amplitudes for $J/\psi \rightarrow \phi f_0^i$ in terms of the production of glueball $|G\rangle$, nonet $|s\bar{s}\rangle$ and $|n\bar{n}\rangle$, via their configuration mixings. Thus, the transition amplitudes can be factorized:

$$M_{J/\psi \rightarrow \phi f_0^i} = \langle f_0^i|G\rangle\langle G|V_\phi|J/\psi\rangle + \langle f_0^i|s\bar{s}\rangle\langle s\bar{s}|V_\phi|J/\psi\rangle$$
$$+ \langle f_0^i|n\bar{n}\rangle\langle n\bar{n}|V_\phi|J/\psi\rangle$$
$$= x_i M_{\phi G} + y_i M_{\phi(s\bar{s})} + z_i M_{\phi(n\bar{n})}. \quad (4)$$

In Fig. 1, the leading diagrams of these transitions are illustrated. For $J/\psi \rightarrow \phi f_0^i$, the subprocesses (a) and (b) are of the same nominal order in perturbative QCD. Thus, we assume $\langle G|V_\phi|J/\psi\rangle \simeq \langle s\bar{s}|V_\phi|J/\psi\rangle$. The transition $M_{\phi(n\bar{n})} = \langle n\bar{n}|V_\phi|J/\psi\rangle$ can only occur via the doubly OZI disconnected process 1(c), which will be of $O(\alpha_s)$ relative to Figs. 1(a) and 1(b) in the perturbative regime. However, due to the complexity of the hadronization of the gluons into $Q\bar{Q}$, the role played by the doubly OZI disconnected diagrams is still not well understood. In particular, the strong mixing of $n\bar{n}$-$s\bar{s}$ in scalar 0^{++} illustrated by the sizable mixings (see later section) shows that Fig. 2 may be expected to occur at similar strength to the singly disconnected diagram, Fig. 1(b). To estimate its contribution, we then introduce another parameter r, which describes the relative strength between the doubly OZI disconnected process and the singly disconnected one such that

$$\langle G|V_\phi|J/\psi\rangle \simeq \langle s\bar{s}|V_\phi|J/\psi\rangle \simeq \frac{1}{\sqrt{2}r}\langle n\bar{n}|V_\phi|J/\psi\rangle, \quad (5)$$

where the factor $\sqrt{2}$ is from the normalization of $n\bar{n}$. In the above equation, we have eventually assumed that the potential is OZI selecting. The left equation holds since

TABLE I. The theoretical reduced partial widths. Parameters α and β are defined as $\alpha \equiv (\cos\phi - \sqrt{2}\sin\phi)/\sqrt{3}$ and $\beta \equiv (\sin\phi + \sqrt{2}\cos\phi)/\sqrt{3}$, where ϕ is the flavor octet-singlet mixing angle between η and η'. Factor γ^2 denotes the invariant decay couplings for $f_0^i \rightarrow PP$. We adopt the same form factors as Refs. [7,8] in the calculations.

|	
$\gamma^2(f_0^i \rightarrow \eta\eta)$	$[\alpha^2 z_i + \sqrt{2}\beta^2 y_i + r_2 x_i + (\sqrt{2}\alpha - \beta)^2 r_3 x_i]^2$
$\gamma^2(f_0^i \rightarrow \eta\eta')$	$2[\alpha\beta(z_i - \sqrt{2}y_i) + (\sqrt{2}\alpha - \beta)(\sqrt{2}\beta + \alpha)r_3 x_i]^2$
$\gamma^2(f_0^i \rightarrow \pi\pi)$	$3[z_i + r_2 x_i]^2$
$\gamma^2(f_0^i \rightarrow K\bar{K})$	$4[\frac{1}{2}(z_i + \sqrt{2}y_i) + r_2 x_i]^2$
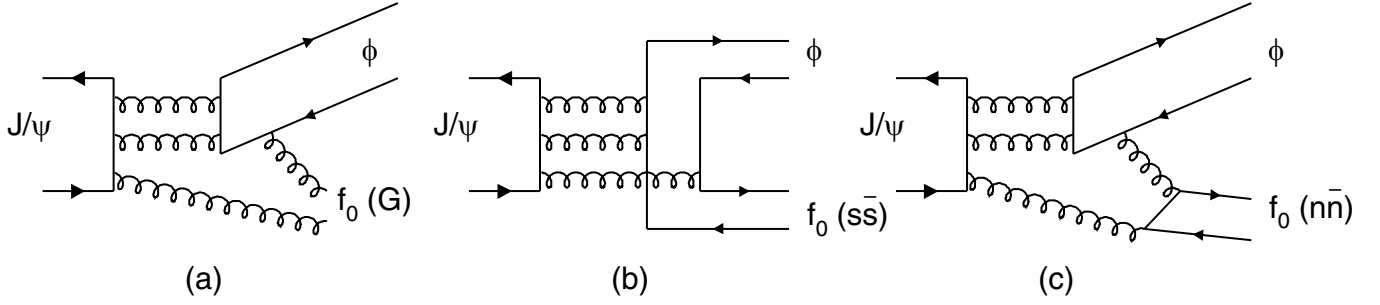
FIG. 1.   Production of f_0^i in $J/\psi \to \phi f_0^i$.

$\langle G|V_\phi|J/\psi \rangle$ and $\langle s\bar{s}|V_\phi|J/\psi \rangle$ both are of the same nominal order and both are singly OZI disconnected. The right equation then distinguishes the doubly OZI disconnected process from the singly disconnected one. It should be noted that contributions from the doubly disconnected processes with the same flavors, such as $\phi f_0(s\bar{s})$ [e.g., replace the $n\bar{n}$ in Fig. 1(c) with $s\bar{s}$], could also contribute in the transition $\langle s\bar{s}|V_\phi|J/\psi \rangle$. However, following the OZI-selection assumption for the transition potentials, such contributions can be regarded as being absorbed into the potential strengths. We will leave the r to be determined by experimental data. Naively, $r \ll 1$ would imply that the doubly disconnected process has a perturbative feature, while $r \simeq 1$ could be a consistency check for the non-perturbative dominance of $n\bar{n}$-$s\bar{s}$ mixing in the 0^{++} channel [19,20].

The above assumption will then allow us to express the partial decay width as

$$\Gamma_{J/\psi \to \phi f_0^i \to \phi PP} = \frac{|\mathbf{p}_{\phi i}|}{|\mathbf{p}_{\phi G}|} \mathrm{BR}_{f_0^i \to PP}[x_i + y_i$$
$$+ \sqrt{2} r z_i]^2 \Gamma_{J/\psi \to \phi G}, \qquad (6)$$

where $\mathbf{p}_{\phi i}$ and $\mathbf{p}_{\phi G}$ are the momenta of the ϕ meson in $J/\psi \to \phi f_0^i$ and the virtual $J/\psi \to \phi G$, respectively. Their ratio gives the kinematic correction for the decays of J/ψ to the ϕ meson and states with different masses, i.e. $M_i \neq M_G$. $\Gamma_{J/\psi \to \phi G} \equiv C_0 |\mathbf{p}_{\phi G}||M_{\phi G}|^2$ is the J/ψ decay
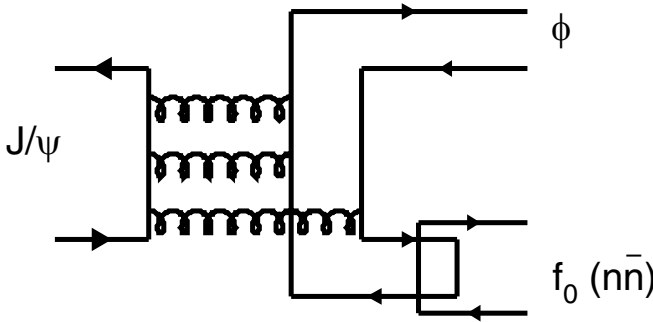
FIG. 2.   Process involves strong mixing of $n\bar{n}$-$s\bar{s}$ in the scalar production. This may occur at similar strength to the singly disconnected Fig. 1(b).

width into ϕ and glueball G, and $|M_{\phi G}|^2$ is the invariant amplitude squared; C_0 is the phase space factor.

Similarly, the transition amplitudes for $J/\psi \to \omega f_0^i$ can be obtained:

$$M_{J/\psi \to \omega f_0^i} = \langle f_0^i|G\rangle\langle G|V_\omega|J/\psi \rangle + \langle f_0^i|s\bar{s}\rangle\langle s\bar{s}|V_\omega|J/\psi \rangle$$
$$+ \langle f_0^i|n\bar{n}\rangle\langle n\bar{n}|V_\omega|J/\psi \rangle$$
$$= x_i M_{\omega G} + y_i M_{\omega(s\bar{s})} + z_i M_{\omega(n\bar{n})}. \qquad (7)$$

Note that here the doubly OZI disconnected process is $M_{\omega(s\bar{s})} = \langle s\bar{s}|V_\omega|J/\psi \rangle$. Also, for the exclusive process $J/\psi \to \omega f_0^i \to \omega PP$, we have the partial decay width

$$\Gamma_{J/\psi \to \omega f_0^i \to \omega PP} = \frac{|\mathbf{p}_{\omega i}|}{|\mathbf{p}_{\omega G}|} \mathrm{BR}_{f_0^i \to PP}[x_i + r y_i$$
$$+ \sqrt{2} z_i]^2 \Gamma_{J/\psi \to \omega G}, \qquad (8)$$

where $\Gamma_{J/\psi \to \omega G} \equiv C_0 |\mathbf{p}_{\omega G}||M_{\omega G}|^2$ is the J/ψ decay width into ω and pure glueball G; $\mathbf{p}_{\omega i}$ and $\mathbf{p}_{\omega G}$ represent the three momenta of the ω meson in $J/\psi \to \omega f_0^i$ and $J/\psi \to \omega G$, respectively. The flavor-blind assumption implies $|M_{\omega G}|^2 = 2|M_{\phi G}|^2$, or equivalently, $2\Gamma_{J/\psi \to \phi G}/|\mathbf{p}_{\phi G}| = \Gamma_{J/\psi \to \omega G}/|\mathbf{p}_{\omega G}|$. For given f_0^i, this relation will allow us to relate the ω and ϕ channel together, and then the parameter r can be determined.

III. NUMERICAL RESULTS

A. Parameters and the f_0^i mass matrix

In this section, we will quantify these subprocesses and investigate the manifestation of the glueball-$Q\bar{Q}$ mixings in the f_0^i production mechanism in the J/ψ decays. As summarized in the Introduction, the recent data for f_0^i production in ψ decays exhibit apparent differences from the simple $Q\bar{Q}$ configurations. It is hence crucial for us to examine that the glueball-$Q\bar{Q}$ mixings obtained in the study of $f_0^i \to PP$ are consistent with the observations in the J/ψ decays. Predictions for the f_0^i productions in $J/\psi \to V f_0^i \to VPP$ will then provide a self-consistent check of this approach.

We first determine the model parameters by fitting the WA102 data [12]. Taking into account the unitarity and

TABLE II. Fitting results in comparison with the data from WA102 and BES. Quantity D denotes $f_0(1370) \to \pi\pi / f_0(1370) \to K\bar{K}$. The differences between these two experimental sets applied for the fittings are highlighted by the bold font.

BR fractions	Data from WA102	Fit-I	Data of WA102 plus BES	Fit-II
D	2.17 ± 0.9	2.34		
$1/D$			0.08 ± 0.08	0.07
$\frac{f_0(1370) \to \eta\eta}{f_0(1370) \to K\bar{K}}$	0.35 ± 0.21	0.62	0.35 ± 0.21	0.17
$\frac{f_0(1500) \to \pi\pi}{f_0(1500) \to \eta\eta}$	5.5 ± 0.84	4.59	5.5 ± 0.84	2.92
$\frac{f_0(1500) \to K\bar{K}}{f_0(1500) \to \pi\pi}$	0.32 ± 0.07	0.41	0.32 ± 0.07	0.42
			0.78 ± 0.66	
$\frac{f_0(1500) \to \eta\eta'}{f_0(1500) \to \eta\eta}$	0.52 ± 0.16	0.68	0.52 ± 0.16	0.73
$\frac{f_0(1710) \to \pi\pi}{f_0(1710) \to K\bar{K}}$	0.20 ± 0.03	0.19	<0.11	0.13
$\frac{f_0(1710) \to \eta\eta}{f_0(1710) \to K\bar{K}}$	0.48 ± 0.14	0.22	0.48 ± 0.14	0.20
$\frac{f_0(1710) \to \eta\eta'}{f_0(1710) \to \eta\eta}$	<0.05 (90% C.L.)	0.03	<0.05 (90% C.L.)	0.03
χ^2		4.6		3.6

orthogonality constraint for the mixing matrix, the data can be fitted with a low reduced χ^2 (see the Fit-I of Table II), and the parameters are presented in Table III. Note that the f_0^i decay branching ratio fractions generally have large errors. It shows that the fraction $\mathrm{BR}(f_0(1710) \to \pi\pi)/\mathrm{BR}(f_0(1710) \to K\bar{K}) = 0.20 \pm 0.03$ with the relatively small errors is the major contribution to χ^2. We also note that the constraints of unitarity and orthogonality will add another 9 relations in the fitting. We arbitrarily require the error to be 3%. Because of this treatment, the absolute values of the χ^2 only provide a reference for the fitting results.

As shown by column Fit-I in Table II, the masses of the $|G\rangle$, $|s\bar{s}\rangle$, and $|n\bar{n}\rangle$ follow the ordering of $M_{s\bar{s}} > M_G > M_{n\bar{n}}$, which is the same as Refs. [7,8]. Furthermore, in this approach we find that the η-η' mixing angle, $\phi = -18.5 \pm 3.1$, fits naturally well the expectations from linear mass relations [21]. It is interesting to see that the sign pattern of the wave function mixing matrix as observed in Ref. [8] is reproduced:

$$|f_0(1710)\rangle = 0.39|G\rangle + 0.91|s\bar{s}\rangle + 0.13|n\bar{n}\rangle,$$
$$|f_0(1500)\rangle = -0.73|G\rangle + 0.37|s\bar{s}\rangle - 0.57|n\bar{n}\rangle, \quad (9)$$
$$|f_0(1370)\rangle = 0.56|G\rangle - 0.12|s\bar{s}\rangle - 0.82|n\bar{n}\rangle,$$

where $|s\bar{s}\rangle$, $|G\rangle$, and $|n\bar{n}\rangle$ are dominant components in $f_0^{1,2,3}$, respectively.

The BES experiment measured the exclusive branching ratios for the f_0^i productions in four channels, $J/\psi \to \phi K\bar{K}$, $\phi\pi\pi$, $\omega K\bar{K}$ and $\omega\pi\pi$. In particular, according to BES [14], $\mathrm{BR}(f_0(1710) \to \pi\pi)/\mathrm{BR}(f_0(1710) \to K\bar{K})$ has an upper limit of 0.11 with 95% confidence level. This ratio, as pointed out earlier, is an important contribution to the χ^2 in the fitting of the WA102 data. For the $f_0(1370)$, the ratio $\mathrm{BR}(f_0(1370) \to K\bar{K})/\mathrm{BR}(f_0(1370) \to \pi\pi) =$

0.08 ± 0.08, is reported, which implies a much smaller $K\bar{K}$ decay rate than its $\pi\pi$ decays. In comparison with the WA102 data, these two ratios provide additional constraints. For the $f_0(1500)$, we derive $\mathrm{BR}(f_0(1500) \to K\bar{K})/\mathrm{BR}(f_0(1500) \to \pi\pi) = (0.8 \pm 0.5)/(1.7 \pm 0.8) \simeq 0.78 \pm 0.66$ by taking the bound values of the numerator and denominator. Although the value overlaps with the WA102 results (0.32 ± 0.07), the large errors will not be helpful for improving the χ^2 in the fitting. We hence include both in the fitting and the parameters and results are presented as Fit-II in Tables II and III to compare with Fit-I.

Again, we find the consistent η-η' mixing angle, $\phi = -22.7 \pm 3.5$ [21]. The same mass ordering, $M_{s\bar{s}} > M_G > M_{n\bar{n}}$, and sign pattern of the mixing matrix are also preserved:

$$|f_0(1710)\rangle = 0.36|G\rangle + 0.93|s\bar{s}\rangle + 0.09|n\bar{n}\rangle,$$
$$|f_0(1500)\rangle = -0.84|G\rangle + 0.35|s\bar{s}\rangle - 0.41|n\bar{n}\rangle, \quad (10)$$
$$|f_0(1370)\rangle = 0.40|G\rangle - 0.07|s\bar{s}\rangle - 0.91|n\bar{n}\rangle,$$

TABLE III. Parameters for the two sets of fittings.

Parameters	Fit-I	Fit-II
ϕ (degree)	-18.5 ± 3.1	-22.7 ± 3.5
M_G (MeV)	1464 ± 47	1519 ± 41
$M_{s\bar{s}}$ (MeV)	1674 ± 10	1682 ± 4
$M_{n\bar{n}}$ (MeV)	1357 ± 23	1304 ± 7
f (MeV)	84 ± 14	71 ± 5
r_2	1.10 ± 0.02	0.88 ± 0.12
r_3	1.12 ± 0.27	1.08 ± 0.20
M_3 (MeV)	1275 ± 34	1260 ± 13

which suggests the consistency between those two sets of data.

To be specific, we abstract some stable features arising from these two fitting results as follows:

(i) Our analysis shows a strong preference of the η-η' mixing angle to be around $-23°--18°$, which is consistent with previous data [21], and should be a good reference for this factorization scheme.

(ii) In the proposed mixing scheme the glueball couplings into isoscalar meson pairs turn out to be strong. This process has a strength of $r_3 \sim 1$ relative to the $Q\bar{Q}$ couplings to the pseudoscalar meson pairs. This suggests the glueball-$Q\bar{Q}$ couplings in the scalar channel at these masses are not perturbative and cautions against a naive pQCD interpretation of the relative importance of Figs. 1(a)–1(c), at least for 0^{++} mesons.

(iii) The same mass ordering, i.e. $M_{s\bar{s}} > M_G > M_{n\bar{n}}$, is found in both of these fitting results as shown in Table III. This is in agreement with the results of Ref. [8]. The mass for the physical $f_0(1370)$ is treated as a free parameter, and we find in Fit-I that $M_3 = 1275 \pm 34$ MeV and in Fit-II, 1260 ± 13. The preference of low masses for the $f_0(1370)$ may be consistent with a recent analysis [13,22]. The analyses of Ref. [13] suggest that the difficulty of separating the $f_2(1270)$ peak from the $f_0(1370)$ led to the difficulty of determining the mass pole position of $f_0(1370)$. Because of the rapid rise of $f_0(1370) \to 4\pi$ phase space with mass, a peak occurring at about 1390 MeV in the 4π channel is actually farther away from the mass pole compared with the $\pi\pi$ channel. Refined analyses show that a pole position around 1315 MeV may be reasonable [22].

(iv) In both fittings the masses of the pure $|s\bar{s}\rangle$ are found to be lower than the physical $f_0(1710)$, which is dominated by the $|s\bar{s}\rangle$ component. Furthermore, the pure $|n\bar{n}\rangle$ are found to be higher than the physical $f_0(1370)$, which is dominated by the $|n\bar{n}\rangle$. This suggests that the glueball mixings lead to a larger mass gap between $f_0(1370)$ and $f_0(1710)$ in comparison with the mass gap between the simple $|n\bar{n}\rangle$ and $|s\bar{s}\rangle$. This is also consistent with the observations that the mass gaps between the $Q\bar{Q}$ dominated axial vectors, $f_1(1285)$ and $f_1(1530)$, and between the tensors, $f_2(1270)$ and $f_2(1525)$, are relatively smaller than that between $f_0(1370)$ and $f_0(1710)$. Furthermore, the relative elevation of the mass of the $f_0(1710)$ relative to the $f_{1,2}(\sim 1530)$ states, in contrast to the similar mass for the low mass states $f_{0,1,2}(1270-1370)$ suggests that the primitive glueball lies in the 1.5–1.7 GeV mass range (this is also in agreement with our analysis of the scalar states, which follows).

(v) The most interesting feature is the stable pattern of the wave function mixing matrix arising from these two fittings, which is essentially determined by the relative mass positions between the pure states ($|G\rangle$, $|s\bar{s}\rangle$, and $|n\bar{n}\rangle$) and physical ones ($M_{1,2,3}$). Note that the mixing elements are given by

$$\begin{cases} x_i = (M_i - M_{s\bar{s}})(M_i - M_{n\bar{n}})C_i, \\ y_i = (M_i - M_{n\bar{n}})fC_i, \\ z_i = \sqrt{2}(M_i - M_{s\bar{s}})fC_i,, \end{cases} \quad (11)$$

where C_i is the normalization factor of Eqs. (9) and (10), and both C_i and f are positive. For the $f_0(1370)$, as an example, the phases can be analytically understood with $M_{s\bar{s}} > M_{n\bar{n}} > M_3$. The same analysis applies to the $f_0(1710)$, where it is essential to have $M_1 > M_{s\bar{s}}$. For the $f_0(1500)$, it shows that M_2 can either be larger or smaller than M_G if both are located between $M_{n\bar{n}}$ and $M_{s\bar{s}}$. This also explains the relative strengths between those components in the wave functions. In particular, all the components are in phase for the $f_0(1710)$; the $|s\bar{s}\rangle$ and $|n\bar{n}\rangle$ are out of phase in the $f_0(1500)$ wave functions ("flavor octet tendency"); for the $f_0(1370)$, the $|n\bar{n}\rangle$ and $|s\bar{s}\rangle$ are in phase and hence have a "flavor singlet tendency." For the last, the significant $|n\bar{n}\rangle$ and negligible $|s\bar{s}\rangle$ turn out to agree with the observation that the $f_0(1370)$ has large branching ratios to $\pi\pi$ and 4π channels.

In brief, we find that the inclusion of the recent BES data does not change the phase patterns of the wave function mixing matrix. The stable phase patterns and relative strengths between the glueball and $Q\bar{Q}$ components can be understood as the preference of the experimental data to have $M_{s\bar{s}} > M_G > M_{n\bar{n}}$ with $1.46 < M_G < 1.52$ GeV. This turns out to be meaningful since such stable mixing patterns possess predictive power, which can be tested in independent processes.

B. Constraints from the $f_0(1710)$ production

The mixing matrices provide a starting point for considering the exclusive decay processes of $J/\psi \to \phi f_0^i \to \phi PP$ and $J/\psi \to \omega f_0^i \to \omega PP$. In particular, the clear signals for $f_0(1710)$ in $J/\psi \to \phi f_0(1710) \to \phi K\bar{K}$ and $J/\psi \to \omega f_0(1710) \to \omega K\bar{K}$ channels [13,14] will allow us to normalize the glueball production rates via Eqs. (6) and (8) in Sec. II B. We will show in this subsection that the f_0^i production in J/ψ decays is correlated with the glueball-$Q\bar{Q}$ mixings introduced in the previous subsection, and a self-consistent treatment of quark-glue couplings is needed. We then clarify that the BES data for the $f_0(1710)$ will provide not only a crucial constraint on the model, but also a self-consistent examination of this approach.

From Eqs. (6) and (8), we have

$$\Gamma_{J/\psi \to \phi f_0^1 \to \phi K\bar{K}} = \frac{|\mathbf{p}_{\phi 1}|}{|\mathbf{p}_{\phi G}|} \mathrm{BR}_{f_0^1 \to K\bar{K}} [x_1 + y_1 + \sqrt{2} r z_1]^2 \Gamma_{J/\psi \to \phi G},$$

$$\Gamma_{J/\psi \to \omega f_0^1 \to \omega K\bar{K}} = \frac{|\mathbf{p}_{\omega 1}|}{|\mathbf{p}_{\omega G}|} \mathrm{BR}_{f_0^1 \to K\bar{K}} [x_1 + r y_1 + \sqrt{2} z_1]^2 \Gamma_{J/\psi \to \omega G}. \quad (12)$$

The BES Collaboration [13] reported the partial decay branching ratio $\Gamma_{J/\psi \to \phi f_0^1 \to \phi K\bar{K}}/\Gamma_{J/\psi}^T = (2.0 \pm 0.7) \times 10^{-4}$, which is consistent with the estimate of the PDG [21] of $(3.6 \pm 0.6) \times 10^{-4}$. For $\Gamma_{J/\psi \to \omega f_0^1 \to \omega K\bar{K}}/\Gamma_{J/\psi}^T$, BES [14] found a much larger ratio $(13.2 \pm 2.6) \times 10^{-4}$ than the PDG [21], $(4.8 \pm 1.1) \times 10^{-4}$, due to better measurement of the $J/\psi \to \omega K\bar{K}$ channel.

As discussed previously, the coupling r determines the role played by the OZI rules for the doubly disconnected processes. It is, in principle, independent of the f_0^i decays, but should be determined by the f_0^i production mechanisms in $J/\psi \to V f_0^i$. To see more clearly the contribution of the doubly OZI disconnected subprocess, we take the naive OZI constraint, $r \to 0$, in the perturbative limit. Follow the implication of the flavor-blind assumption: $2\Gamma_{J/\psi \to \phi G}/|\mathbf{p}_{\phi G}| = \Gamma_{J/\psi \to \omega G}/|\mathbf{p}_{\omega G}|$, and take the ratio between the ϕ and ω channels in Eq. (12), we then have

$$R_{\text{OZI}} = \frac{\Gamma_{J/\psi \to \phi f_0^1 \to \phi K\bar{K}}}{\Gamma_{J/\psi \to \omega f_0^1 \to \omega K\bar{K}}} = \frac{|\mathbf{p}_{\phi 1}|}{|\mathbf{p}_{\omega 1}|} \frac{[x_1 + y_1]^2}{2[x_1 + \sqrt{2}z_1]^2} \simeq 3.0,$$

$$(13)$$

which is contradicted by the experimental result $R_{\text{exp}} = 0.15$ from BES [13,14] and $R_{\text{exp}} = 0.75$ from PDG [21].

A solution is to keep the flavor-blind assumption, but allow $r \neq 0$, i.e. to include contributions from Fig. 1(c). With the experimental data for the $f_0(1710)$ production, we can determine the coupling strength r:

$$r = \frac{1}{\chi_0 y_1 - \sqrt{2}z_1} [(1 - \chi_0)x_1 + y_1 - \sqrt{2}\chi_0 z_1], \quad (14)$$

where $\chi_0 \equiv (2R_{\text{exp}}|\mathbf{p}_{\omega 1}|/|\mathbf{p}_{\phi 1}|)^{1/2}$. Note that R_{exp} is determined by the experimental data; r is not a free parameter in this calculation. We find that for $R_{\text{exp}} = 0.15$–0.75, r has a range of 0.5–2.5, which suggests a rather strong contribution from the doubly OZI disconnected diagram. It shows that though there are significant discrepancies between the PDG estimates and BES measurements, they both favor large values for r and breaking of the OZI rule. In particular, this range is within the expectation of nonperturbative glueball-$Q\bar{Q}$ couplings as found in the configuration mixing scheme for the f_0 states, and as suggested by the parameters r_2 and r_3 in Sec. II. In this sense, the value $r \sim 1$ turns out to be a self-consistent result of this model.

To test the self-consistency of the calculation and sensitivity of other branching ratios to r, we examine the following four cases: (i) with the parameters of Fit-I, and $R_{\text{exp}} = 0.75$ from the PDG [21], we derive $r = 0.5$ and the predictions are labeled as Fit-I(a); (ii) with the parameters of Fit-I, and $R_{\text{exp}} = 0.15$ from the BES [13,14], we derive $r = 2.5$ and the predictions are labeled as Fit-I(b); (iii) with the parameters of Fit-II, and $R_{\text{exp}} = 0.75$, we

derive $r = 0.6$ and the predictions are labeled as Fit-II(a); (iv) with the parameters of Fit-II, and $R_{\text{exp}} = 0.15$, we derive $r = 2.2$ and the predictions are labeled as Fit-II(b). Recalling that Fit-II has accommodated the data from BES, we note in advance that Fit-II(b) is the only set where the new experimental data from BES have been used throughout. We hence would expect that predictions from Fit-II(b) are the self-consistent ones.

With a fixed $R_{\text{exp}} = \Gamma_{J/\psi \to \phi f_0^1 \to \phi K\bar{K}}/\Gamma_{J/\psi \to \omega f_0^1 \to \omega K\bar{K}}$, we are able to normalize the glueball production widths via Eqs. (12) and (14). In particular, the spin-averaged invariant amplitudes squared are

$$|M_{\phi G}|^2 = \frac{1}{2}|M_{\omega G}|^2 = \frac{\Gamma_{J/\psi \to \phi G}}{|\mathbf{p}_{\phi G}|}$$

$$= \frac{\Gamma_{J/\psi \to \phi f_0^1 \to \phi K\bar{K}}}{|\mathbf{p}_{\phi 1}|\text{BR}_{f_0^1 \to K\bar{K}}[x_1 + y_1 + \sqrt{2}rz_1]^2}, \quad (15)$$

where the ratio $\text{BR}_{f_0^1 \to K\bar{K}} \equiv \Gamma(f_0(1710) \to K\bar{K})/\Gamma(f_0(1710) \to \text{all})$ will be estimated based on the present experimental information. So far, the experimental evaluations of $\text{BR}_{f_0^1 \to K\bar{K}}$ still have large uncertainties. Earlier analyses from Ref. [23] gave $\text{BR}_{f_0^1 \to K\bar{K}} = 0.38$, which however may not be reliable. Taking into account that $K\bar{K}$ is the dominant decay mode for the $f_0(1710)$, and the branching ratio fractions of other pseudoscalar pair ($\pi\pi$, $\eta\eta$, $\eta\eta'$) decays over $K\bar{K}$ are small [12,13], a more reliable estimate could be $\text{BR}_{f_0^1 \to K\bar{K}} \simeq \Gamma(f_0(1710) \to K\bar{K})/\Gamma(f_0(1710) \to (K\bar{K} + \pi\pi + \eta\eta + \eta\eta')) \simeq 0.60$ with the WA102 data. We have also assumed that the 4π decay channel is negligible [22].

A large value of $\text{BR}_{f_0^1 \to K\bar{K}} = 0.60$ will predict different glueball production rates. However, we would like to point out in advance that the magnitudes of the predicted glueball production rates and the predicted branching ratios for the $f_0(1500)$ and $f_0(1370)$ will not change drastically with the change of $\text{BR}_{f_0^1 \to K\bar{K}}$ from 0.38 to 0.60, or even up to 0.8. This is natural since the underlying physics in the exclusive process of $J/\psi \to V f_0^i$ should not be sensitive to the experimental uncertainties arising from the total widths of the f_0^i. We will come back to this point in the next subsection. To proceed, we will then adopt $\text{BR}_{f_0^1 \to K\bar{K}} = 0.60$ in the calculations.

C. Predictions for the glueball, $f_0(1500)$ and $f_0(1370)$

With $\text{BR}_{f_0^1 \to K\bar{K}} = 0.60$, we have access to the normalized invariant amplitudes squared for the glueball production via Eq. (15). The branching ratios for $J/\psi \to VG$ can then be derived, and the results are presented in Table IV for the four circumstances defined above.

Although there exist uncertainties due to dependence on the experimental data for $\text{BR}_{f_0^1 \to K\bar{K}}$, we find that the magnitudes are well constrained at order 10^{-4}. Interestingly,

the partial width of $J/\psi \rightarrow \omega G$ is predicted to be larger than $J/\psi \rightarrow \phi G$ by about a factor of 2. A well-determined value for R_{exp} will improve the accuracy of this prediction. Meanwhile, it is interesting to compare this approach with the one proposed in Ref. [18]. In the latter, the pQCD assumption provided a way to connect the electromagnetic decay processes with the strong decays via gluon-counting rules to the next-to-leading order, through which the glueball production rate can be estimated. However, the estimate strongly depended on the validity of treating all the exchanged gluons as perturbative. In contrast, the validity of pQCD treatment in this work can be examined by the factorization scheme and controlled by the experimental data. It is worth noting, since the doubly OZI disconnected processes are intimately related to the glueball-$Q\bar{Q}$ mixings, it is not surprising that nonperturbative contributions are still significant in $J/\psi \rightarrow V f_0^i$.

As follows, we will examine the predictions from those four circumstances for the production of the $f_0(1500)$ and $f_0(1370)$, and compare them with the available experimental data from BES.

To calculate the partial decay widths for $J/\psi \rightarrow V f_0^i \rightarrow VPP$, we still need the branching ratios for $f_0^i \rightarrow PP$. For $f_0^i \rightarrow K\bar{K}$ and $\pi\pi$, the experimental data from PDG are listed in Table V. Some of these values still have large uncertainties. However, we note that the branching ratio fractions, $\text{BR}(J/\psi \rightarrow \phi f_0^i \rightarrow \phi PP)/\text{BR}(J/\psi \rightarrow \omega f_0^i \rightarrow \omega PP)$, are independent of the branching ratios for $f_0^i \rightarrow PP$. Therefore, the theoretical predictions for the J/ψ decay branching ratio fractions can still be compared with the experimental data. Again, we note that the predicted physics for the exclusive $J/\psi \rightarrow V f_0^i$ should not be dramatically sensitive to the uncertainties arising from the branching ratios for $f_0^i \rightarrow PP$.

As summarized earlier, the BES results [13] show that the branching ratios for $J/\psi \rightarrow \phi f_0^i \rightarrow \phi\pi\pi$ are sizable for $f_0(1370)$ and $f_0(1500)$, while the $f_0(1710)$ is negligible. In $J/\psi \rightarrow \phi f_0^i \rightarrow \phi K\bar{K}$, the situation changes, and the $f_0(1710)$ has the clearest signals. On the other hand, signals for the $f_0(1370)$ and $f_0(1500)$ in $\omega\pi\pi$ and $\omega K\bar{K}$

TABLE V. Experimental values for the branching ratios of $f_0^i \rightarrow PP$. For $\text{BR}_{f_0(1710)\rightarrow\pi\pi}$ and $\text{BR}_{f_0(1370)\rightarrow K\bar{K}}$, we apply the results from the BES Collaboration [13,14].

$\text{BR}_{f_0^i \rightarrow PP}$	$K\bar{K}$	$\pi\pi$
$f_0(1710)$	0.60	$0.60 \times 11\%$
$f_0(1500)$	0.086	0.349
$f_0(1370)$	$0.20 \times 10\%$	0.20

are found to be small and difficult to isolate, while they are relatively clear in $\phi\pi\pi$ and $\phi K\bar{K}$.

In Table VI, the branching ratios for the J/ψ decays into $\phi K\bar{K}$, $\omega K\bar{K}$, $\phi\pi\pi$, and $\omega\pi\pi$ via the f_0^i are presented for Fit-I(a), Fit-I(b), Fit-II(a), and Fit-II(b). It shows that Fit-I(a) and Fit-II(a) with $R_{\text{exp}} = 0.75$ lead to sizable branching ratios for the $f_0(1500)$ in $\omega\pi\pi$. Therefore, they are not favored by the BES observations. This should not be surprising since BES is in favor of $R_{\text{exp}} = 0.15$.

In contrast, Fit-I(b) and Fit-II(b) with $R_{\text{exp}} = 0.15$ produce consistent patterns for $f_0(1500)$ and $f_0(1370)$. The $f_0(1710)$ branching ratios in both $(\omega)\pi\pi$ and $(\phi)\pi\pi$ are found significantly smaller than in $(\omega)K\bar{K}$ and $(\phi)K\bar{K}$, respectively. With a large branching ratio of $(13.2 \pm 2.6) \times 10^{-4}$ for $J/\psi \rightarrow \omega f_0(1710) \rightarrow \omega K\bar{K}$ as input, we obtain the corresponding ratio 1.45×10^{-4} for $J/\psi \rightarrow \omega f_0(1710) \rightarrow \omega\pi\pi$. This quantity seems quite big, and implies that it could be relatively easy to separate the $f_0(1710)$ signal in the $\omega\pi\pi$ channel than both $f_0(1500)$ and $f_0(1370)$. However, taking into account that the $\pi\pi/K\bar{K}$ ratio still has large uncertainties, e.g., BES gives an upper limit of 0.11 with 90% C.L., the branching ratio of $J/\psi \rightarrow \omega f_0(1710) \rightarrow \omega\pi\pi$ can be further suppressed with smaller $\pi\pi/K\bar{K}$ ratios. The $f_0(1500)$ has sizable branching ratios in $(\phi)\pi\pi$, while all the other channels are small, especially the ones in association with ω production. It is worth noting that an upper limit on $J/\psi \rightarrow \omega f_0(1500)$ is given by BES at 0.9×10^{-4} [24]. Adding the branching ratios of $(\omega)K\bar{K}$ and $(\omega)\pi\pi$ for the $f_0(1500)$, the ratios are well below the limit, which is in agreement with the data. Comparing Fit-I(b) with Fit-II(b) for the $f_0(1370)$, we find that the large uncertainties arising from the $K\bar{K}$ to $\pi\pi$ ratios do not change the major character of the branching ratio pattern. Its branching ratios in $(\phi)\pi\pi$ are significantly bigger than in $(\omega)\pi\pi$, which was previously regarded as a "puzzle" for this state.

As manifested by Eq. (14), a small value for R_{exp} such as 0.15, corresponds to $r \sim 2.2$, which implies strong nonperturbative contributions from the doubly disconnected processes. We stress again that r is not a free parameter in this model. It is determined by the experimental measurement of R_{exp} for the $f_0(1710)$, while all the other variables in Eq. (14) are from either kinematics or the independently determined mixing matrix elements. Therefore, the ratio R_{exp} also provides a good test of r, which is in a reasonable

TABLE IV. Normalized branching ratios for the glueball production in $J/\psi \rightarrow \phi G$ and $J/\psi \rightarrow \omega G$. The four sets of calculations correspond to Fit-I(a): with the parameters fitted by Fit-I, and $R_{\text{exp}} = 0.75$ from the PDG [21]; Fit-I(b): with the parameters fitted by Fit-I, and $R_{\text{exp}} = 0.15$ from the BES [13,14]; Fit-II(a): with the parameters fitted by Fit-II, and $R_{\text{exp}} = 0.75$; and Fit-II(b): with the parameters fitted by Fit-II, and $R_{\text{exp}} = 0.15$. We note that Fit-II(b) is the one treating the experimental data self-consistently.

BR for G ($\times 10^{-4}$)	Fit-I(a)	Fit-I(b)	Fit-II(a)	Fit-II(b)
$\text{BR}_{J/\psi \rightarrow \phi G}$	3.97	1.36	3.96	1.63
$\text{BR}_{J/\psi \rightarrow \omega G}$	9.02	3.09	9.11	3.75

TABLE VI.   Predictions for $\mathrm{BR}_{J/\psi \to V f_0^i \to VPP}$ in comparison with the available experimental data. The BES results [13,14] are quoted in the round brackets, while the PDG results [21] are quoted in the square brackets. The symbol "$\cdots$" means that signals of the corresponding states have not been observed in the BES experiment. See the caption of Table IV for definitions of these four sets.

Fit-I(a)	$K\bar{K}(\phi)$	Data	$K\bar{K}(\omega)$	Data	$\pi\pi(\phi)$	Data	$\pi\pi(\omega)$	
$f_0(1710)$ ($\times 10^{-4}$)	3.60	$[3.6 \pm 0.6]$	4.80	$[4.8 \pm 1.1]$	0.40	$\cdots$	0.53	$\cdots$
$f_0(1500)$ ($\times 10^{-4}$)	0.19	(0.8 ± 0.5)	1.38	$\cdots$	0.77	(1.7 ± 0.8)	5.60	$\cdots$
$f_0(1370)$ ($\times 10^{-4}$)	0.00	(0.3 ± 0.3)	0.08	$\cdots$	0.01	(4.3 ± 1.1)	0.83	$\cdots$
Fit-I(b)	$K\bar{K}(\phi)$	Data	$K\bar{K}(\omega)$	Data	$\pi\pi(\phi)$	Data	$\pi\pi(\omega)$	
$f_0(1710)$ ($\times 10^{-4}$)	2.00	(2.0 ± 0.7)	13.20	(13.2 ± 2.6)	0.22	$\cdots$	1.45	$\cdots$
$f_0(1500)$ ($\times 10^{-4}$)	0.66	(0.8 ± 0.5)	0.09	$\cdots$	2.67	(1.7 ± 0.8)	0.35	$\cdots$
$f_0(1370)$ ($\times 10^{-4}$)	0.19	(0.3 ± 0.3)	0.05	$\cdots$	1.93	(4.3 ± 1.1)	0.54	$\cdots$
Fit-II(a)	$K\bar{K}(\phi)$	Data	$K\bar{K}(\omega)$	Data	$\pi\pi(\phi)$	Data	$\pi\pi(\omega)$	
$f_0(1710)$ ($\times 10^{-4}$)	3.60	$[3.6 \pm 0.6]$	4.80	$[4.8 \pm 1.1]$	0.40	$\cdots$	0.53	$\cdots$
$f_0(1500)$ ($\times 10^{-4}$)	0.23	(0.8 ± 0.5)	1.20	$\cdots$	0.92	(1.7 ± 0.8)	4.85	$\cdots$
$f_0(1370)$ ($\times 10^{-4}$)	0.01	(0.3 ± 0.3)	0.18	$\cdots$	0.14	(4.3 ± 1.1)	1.81	$\cdots$
Fit-II(b)	$K\bar{K}(\phi)$	Data	$K\bar{K}(\omega)$	Data	$\pi\pi(\phi)$	Data	$\pi\pi(\omega)$	
$f_0(1710)$ ($\times 10^{-4}$)	2.00	(2.0 ± 0.7)	13.20	(13.2 ± 2.6)	0.22	$\cdots$	1.45	$\cdots$
$f_0(1500)$ ($\times 10^{-4}$)	0.46	(0.8 ± 0.5)	0.13	$\cdots$	1.89	(1.7 ± 0.8)	0.52	$\cdots$
$f_0(1370)$ ($\times 10^{-4}$)	0.26	(0.3 ± 0.3)	0.09	$\cdots$	2.63	(4.3 ± 1.1)	0.94	$\cdots$

range between 0.5 to 2.2 in line with strong QCD ("nonperturbative QCD").

Interestingly, we also find that for much smaller R_{exp}, hence larger r, the production branching ratios for $f_0(1500)$ and $f_0(1370)$ via $\omega\pi\pi$ will increase and worsen the predictions. In this sense, we identify that the strong contributions from the doubly OZI disconnected processes are not an artificial effect. The preferred coupling strength is consistent with the expectation of a nonperturbative glueball-$Q\bar{Q}$ interaction appearing in the configuration mixings. It also suggests that an accurate measurement of R_{exp} for the $f_0(1710)$ [13,14] will be crucial for the study of the reaction mechanisms.

IV. SUMMARY AND PERSPECTIVE

In this work, we proposed a factorization scheme for the study of the scalar mesons f_0^i production in the J/ψ hadronic decays into the isoscalar vector mesons V ($= \phi$ and ω) and pseudoscalar meson pairs PP ($= \pi\pi$, $K\bar{K}$, $\eta\eta$, and $\eta\eta'$), i.e. $J/\psi \to V f_0^i \to VPP$. With an improved treatment for the glueball-$Q\bar{Q}$ mixing in the configuration of the f_0^i, we found that the reaction mechanisms were very sensitive to the structure of the f_0^i. In particular, due to the glueball-$Q\bar{Q}$ mixing, the predicted branching ratios for $J/\psi \to V f_0^i \to VPP$ exhibit unusual patterns, which are in agreement with the experimental data from BES.

The importance of glueball-$Q\bar{Q}$ mixing is also highlighted by the indispensible contributions from the doubly disconnected processes, which turn out to be nonperturbative and violate the OZI rule. Since the coupling $gg \to Q\bar{Q}$ in the doubly disconnected processes is essentially the

same as the glueball-$Q\bar{Q}$ mixing, the nonperturbative feature of the doubly disconnected processes is self-consistent with the proposed configuration mixing scheme for these three f_0 states. In this sense, our results not only provide an understanding of the recent puzzling experimental data from BES [13–15], but also highlight the strong possibility of the existence of glueball contents in the $f_0(1500)$, and its sizable interferences in $f_0(1710)$. Furthermore, due to the configuration mixing, the $|n\bar{n}\rangle$ dominant $f_0(1370)$ tends to have a lower mass lower than 1370 MeV, which also agrees with a recent more refined analysis [13,22].

With Eqs. (9) and (10), and applying the method of Ref. [6], the relative decay widths (excluding phase space) for $f_0^i \to \gamma\gamma$ are found to be $f_0(1370):f_0(1500): f_0(1710)$–12:2:1. The results are consistent with those of Ref. [6], which should not be surprising since the mixing matrices are similar to each other.

In this factorization scheme, a quantitative normalization of the scalar glueball production rate in the $J/\psi \to VG$ is also accessible. With the pure glueball mass in a range of 1.46–1.52 GeV, we obtain the branching ratios $\mathrm{BR}_{J/\psi \to \phi G} \simeq \frac{1}{2} \mathrm{BR}_{J/\psi \to \omega G} \simeq (1 \sim 2) \times 10^{-4}$. Although a direct measurement of the glueball production seems impossible, the success of this approach provides a key for understanding the recently claimed signals for another scalar $f_0(1790)$. This state is found distinguished from the $f_0(1710)$ based on two observations [15,22]: (i) the $f_0(1710)$ has clear signals in $(\omega)K\bar{K}$ and $(\phi)K\bar{K}$, while the $f_0(1790)$ is not visible; (ii) there is a definite peak in $\phi\pi\pi$ for the $f_0(1790)$, while the signal for $f_0(1710)$ is negligible. As a result, the branching ratios between $K\bar{K}$ and $\pi\pi$ are larger than a factor of 20. These distinguished features

suggest that the $f_0(1790)$ may be a radial excited state dominated by $|n\bar{n}\rangle$ which appears not to be strongly mixed with the ground state.

As pointed out in Ref. [25], the decays $J/\psi \rightarrow \gamma f_0 \rightarrow \gamma\gamma V$, where $V = \omega$, ϕ, and ρ^0, can provide further independent information about the f_0 states. Using the discussions of Ref. [6], we find the widths for $J/\psi \rightarrow \gamma f_0^i$ satisfy $f_0(1710) > f_0(1500) > f_0(1370)$, which is also consistent with the BES data. Further improved statistics at BES for these f_0 states in both hadronic and radiative decays should be able to quantize the model predictions, and provide us with more information about their structures.

[1] F. E. Close and N. A. Tornqvist, J. Phys. G **28**, R249 (2002).

[2] S. J. Brodsky, A. S. Goldhaber, and J. Lee, Phys. Rev. Lett. **91**, 112001 (2003).

[3] K. Abe *et al.* (Belle Collaboration), Phys. Rev. Lett. **89**, 142001 (2002).

[4] C. Morningstar and M. Peardon, Phys. Rev. D **56**, 4043 (1997).

[5] G. Bali *et al.* (UKQCD Collaboration), Phys. Lett. B **309**, 378 (1993).

[6] F. E. Close, G. R. Farrar, and Z. Li, Phys. Rev. D **55**, 5749 (1997).

[7] F. E. Close and C. Amsler, Phys. Lett. B **353**, 385 (1995); Phys. Rev. D **53**, 295 (1996).

[8] F. E. Close and A. Kirk, Phys. Lett. B **483**, 345 (2000).

[9] D. V. Bugg, M. Peardon, and B. S. Zou, Phys. Lett. B **486**, 49 (2000).

[10] X. Y. Shen *et al.* (BES Collaboration), hep-ex/0209031.

[11] P. Minkowski and W. Ochs, Nucl. Phys. B Proc. Suppl. **121**, 123 (2003); W. Ochs, AIP Conf. Proc. **717**, 295 (2004).

[12] D. Barberis *et al.*, Phys. Lett. B **479**, 59 (2000).

[13] M. Ablikim *et al.* (BES Collaboration), Phys. Lett. B **607**, 243 (2005).

[14] M. Ablikim *et al.* (BES Collaboration), Phys. Lett. B **603**, 138 (2004).

[15] S. Jin, in *Proceedings of the 32nd International Conference on High-Energy Physics (ICHEP2004), Beijing, 2004* (World Scientific, Singapore, 2004).

[16] S. Okubo, Phys. Lett. **5**, 1975 (1963); G. Zweig, in *Development in the Quark Theory of Hadrons*, edited by D. B. Lichtenberg and S. P. Rosen (Hadronic Press, MA, 1980); J. Iizuka, Prog. Theor. Phys. Suppl. **37**, 38 (1966).

[17] A. Seiden, H. F.-W. Sadrozinski, and H. E. Haber, Phys. Rev. D **38**, 824 (1988).

[18] F. E. Close and Q. Zhao, Phys. Lett. B **586**, 332 (2004).

[19] P. Geiger and N. Isgur, Phys. Rev. D **47**, 5050 (1993).

[20] H. J. Lipkin and B. S. Zou, Phys. Rev. D **53**, 6693 (1996).

[21] S. Eidelman *et al.* (Particle Data Group), Phys. Lett. B **592**, 1 (2004).

[22] D. V. Bugg (private communication).

[23] R. C. Longacre *et al.*, Phys. Lett. B **177**, 223 (1986).

[24] M. Ablikim *et al.* (BES Collaboration), Phys. Lett. B **598**, 149 (2004).

[25] F. E. Close, in *Proceedings of the 32nd International Conference on High-Energy Physics (ICHEP2004), Beijing, 2004* (Ref. [15]).